

Article

Hydrothermal Conversion of Waste Biomass from Greenhouses into Hydrochar for Energy, Soil Amendment, and Wastewater Treatment Applications

Abu-Taher Jamal-Uddin ¹, Shakirudeen A. Salaudeen ², Animesh Dutta ¹ and Richard G. Zytner ^{1,*}

¹ School of Engineering, University of Guelph, Guelph, ON N1G 2W1, Canada; ajamalud@uoguelph.ca (A.-T.J.-U.); adutta@uoguelph.ca (A.D.)

² Faculty of Sustainable Design Engineering, University of Prince Edward Island, Charlottetown, PE C1A 4P3, Canada; ssalaudeen@upe.ca

* Correspondence: rzytner@uoguelph.ca

Abstract: Solid hydrochar (HC) produced by hydrothermal carbonization (HTC) of tomato plant biomass from a greenhouse (GH) was assessed for different inhouse applications, including fuel, seed germination, and leached GH nutrient feed (GNF) wastewater treatment. Completed experiments showed encouraging results. HC was revealed to be an efficient renewable fuel, having peat-like characteristics with high heating value of about 26.0 MJ/kg and very low clinker forming potential. This would allow the use of HC as fuel for GH heating as a substitute to costly natural gas, or it could be commercialized after pelletizing. Experiments with soil application showed substantial potential for the produced HC in better seed germination of tomato plants. Another benefit from use of the produced HC is as a soil additive, which would also contribute to environmental emission reduction. Results suggest that the generated HC can remove about 6–30% of nutrients from leached-GNF wastewater. This would be an essential treatment in the reduction of nutrients from leached water from GH operations, and thus could prevent/reduce eutrophication. The exhausted HC after treatment application could then be reused for soil remediation. Overall, the paper highlights the potential applications of hydrothermal treatment in valorization of low-valued GH TPB waste, resulting in a circular economy.

Keywords: tomato plant biomass; hydrothermal carbonization; characterization; soil remediation; adsorption; leached nutrient water treatment



Citation: Jamal-Uddin, A.-T.; Salaudeen, S.A.; Dutta, A.; Zytner, R.G. Hydrothermal Conversion of Waste Biomass from Greenhouses into Hydrochar for Energy, Soil Amendment, and Wastewater Treatment Applications. *Energies* **2022**, *15*, 3663. <https://doi.org/10.3390/en15103663>

Academic Editor: Elena Rada

Received: 14 April 2022

Accepted: 9 May 2022

Published: 17 May 2022

Publisher's Note: MDPI stays neutral with regard to jurisdictional claims in published maps and institutional affiliations.



Copyright: © 2022 by the authors. Licensee MDPI, Basel, Switzerland. This article is an open access article distributed under the terms and conditions of the Creative Commons Attribution (CC BY) license (<https://creativecommons.org/licenses/by/4.0/>).

1. Introduction

Nutrient contaminated runoff of agricultural activities from the USA and Canada increase algae growth in Lake Erie. In 2015, the nutrient load was the highest in 100 years for negatively impacting aquatic inhabitants, leading to the potential failure of Lake Erie. Thus, both countries are implementing different initiatives to control this historic eutrophication problem [1].

One of the initiatives in Ontario involves regulating nutrient-based biomass and leached greenhouse (GH) nutrient (GNF) wastewater, which is restricted to land disposal without treatment. About 95% of Ontario GHs are located in the southern part and most of them are tomato GHs producing about 0.4 million t/y of exportable tomatoes [2]. Consequently, waste tomato plant biomass (TPB) must be treated and reused.

Biomass is a lignocellulosic material that includes forest and agricultural waste, sewage sludge, food waste etc. These materials have good potential to be used in biorefineries and other processing steps. Most of the biomass, including agricultural, forest, and greenhouse (GH), have inferior physicochemical properties, such as poor homogeneity, high moisture content, hydrophilic nature, poor grindability, high alkalinity and alkaline earth metal content, and low bulk energy density [3]. This inferior quality results in lower

heating value, high ash content with low combustion efficiency (due to slug formation), and high cost of pre-drying and processing by conventional techniques, including torrefaction, pyrolysis, gasification, and liquefaction. All these treatment options involve high temperature processes, which cause complications, along with limitations, when treating biomass with high moisture (water content) [4]. Among the developed technologies to pretreat biomass, hydrothermal carbonization (HTC), also referred to as wet torrefaction, is used in this study. It is an alternative to the traditional conversion method and is a convenient and promising technique, due to its adaptability to moisture content and varied biomass compositions [5,6].

The chemical characteristics of biomass composition consist of cellulose (30–60%), hemicellulose (20–40%), and lignin (1–25%) [7]. Biomass also contains a wide range and concentration of extractives, including fats, waxes, phenols, lignans, flavonoids, proteins, gums, resins, etc. [8,9] Cellulose is a linear and crystalline homopolymer of repeating d-glucose subunits called cellobiose, consisting of two glucoses linked by β -1,4 glycosidic bonds. Hemicellulose is mostly connected to lignin within the plant with covalent links and is thus fixed in fiber structure. Lignin is a high molecular-weight, water insoluble, hydrophobic cross-branched plant polymer having complex and variable structures. It is present in the plant cell wall and covalently binds hydrogen in compounds, such as ether, ester, glycosidic acid, with cellulose and hemicellulose, giving mechanical strength to the plant [10].

The interest in finding uses for agricultural biomass, including GH biomass, has been driven by an increase in fuel costs [11] and positive environmental benefits, as outlined in environmental commitments to address global warming due to CO₂ emissions [12]. Biomass has multifaceted potential, including its transformation to biofuels as replacement for fossil-based fuel sources or conversion into highly valuable green carbon. The conversion of densified lignocellulosic biomass into solid fuel pellets would allow it to become an industrial commodity in the fuel market. Furthermore, the densification of biomass helps overcome handling limitations, enhances density, and offers uniformity of particle size and shape, and saves on costs of transportation [13].

Biomass has potential to be transformed into hydrocarbon fuels, such as bioethanol, biobutanol, bio-oil biodiesel, algal-oil, hydrogen, biomethane, and aviation fuel [7].

Roman et al. [14] investigated the influence of biomass micronization with 8 biomass waste (sunflower husk, oat husk, wheat straw, miscanthus, hay, wood chips, willow, and poplar) as fuel for heat and electricity generation, replacing conventional coal [14]. In addition to fuel, there are advanced applications of biomass, including carbon black and activated carbon, which require high carbon content (>40–75%), high porosity, and high N and S contents, along with other application-specific requirements [15,16]. The simplicity of hydrothermal carbonization (HTC) in generating HC from readily available biomass involves activation without any demineralization steps. HC has multiple potential applications, including: (i) gasification to produce gas energy, (ii) soil remediation application [17], (iii) activated carbon wide applications in engineering and wastewater treatment [7], (iv) generation of nanocomposites with other materials (v) significant contribution to securing green energy, as it can help in retaining nutrients in soil and supplying nutrients to plant growth and it could also decrease emissions, saving the environment.

Among thermal processes, torrefaction (200–300 °C) treatment is conventionally conducted to increase energy density, grindability, hydrophobicity, and to dry biomass [18]. Pyrolysis is a thermal treatment (300–800 °C) conducted in an inert atmosphere (N₂) to reduce volatile matter from organics and increase carbon content [19]. Pyrolysis is mostly used for biofuels (chemicals) and char from carbonaceous feedstock. It is based on a slow heating rate. Hydrothermal carbonization (HTC) is conducted at a lower temperature (180–260 °C) in a sub-critical water temperature region using any category of biomass (wet with high water), by adding water. HTC converts organic matter in biomass into mostly carbon-dense hydrochar (HC), liquid and minor gases in the absence of oxygen. HC

properties differ significantly, due to the diversity of feedstock and the complexity in HTC reactions, and need characterization.

The chemical transformations that occur during the HTC pretreatment process include hydrolysis, dehydration, decarboxylation, decomposition, condensation, bond cleavage, formation of new bonds, and isomerization of hemicellulose, cellulose, and lignin derivatives [20,21]. Water initiates the hydrolysis reaction by lowering the activation energy level that transforms hemicellulose and cellulose, producing oligomers and monomers [22]. However, water replaces the toxic and corrosive agents, which is a positive side of the water medium at this stage [23,24]. HTC process water is supposed to contain some aromatics, and phenolic and furan derivatives, such as furfural and 5-hydroxymethyl furfural (5HMF), and carboxylic acid, along with other organic acids. The HMF and levulinic acid have been identified by the US Department of Energy (DOE) as within the “top 12” value-added chemicals from biomass. They have very high heating value (HHV) [25]. Acids formed during the HTC process work as self-catalysts to improve hydrochar surface quality [26]. Basic catalysts promote 5 hydroxymethyl furfural (HMF) [27], and increase concentrations of acids (formic, lactic, and acetic acids), as well as sugars, in process water [28].

Other high temperature processes are hydrothermal liquefaction (HTL), which operates at 280–340 °C [29], and hydrothermal gasification (HTG), which occurs at above the critical water temperature, 374 °C [30]. HTG is also termed super critical water gasification (SCWG) [31,32]. As HTL and HTG are high temperature (>300 °C) and pressure (>2000 psi) processes, they involve higher operational costs, along with handling complications, as compared to the HTC process. HTC gets much attention as a method of transformation for organic waste materials into important and value-added solid products, including liquid (aqua) chemicals [33]. Research activities are increasingly focused on the use of HTC for handling low-grade biomass. HTC handles high moisture containing biomass at lower temperatures (200–260 °C, 2–5 MPa). However, no work has been conducted on wet TPB. A study reported the pyrolysis of agricultural field dry tomato residue (leaf, stem, tomato) after harvest at 400 °C and the derived char was used as soil remediation [34].

In light of the operational simplicity and low heating costs, HTC is recognized to be a potential process for the treatment of GH wet TPB in this study at lower temperatures (180–260 °C). Solid HC produced at temperatures >180 °C will kill (sterilize) pathogenic species in the biomass if present. It has additional use for promoting crop growth through its high nutrient content [35]. Hydrochar has H/C and O/C ratios almost like peat [22], providing prime value as a fuel. When using the HTC process, there is no need to worry about biomass high moisture content as water is normally added as reaction media. Accordingly, the high moisture (water) content in tomato plant waste biomass makes HTC treatment well suited for the conversion of the biomass into HC.

Experiments were conducted to assess the recycle potential of greenhouse (GH) biomass by converting it into value-added products. Review of literature reveals negligible work on hydrothermal production of HC from TPB at lower temperatures (220–260 °C) to simplify the production. The completed study characterized the properties of the TPB, the main product HC, and the by-products to ensure their beneficial applications to GH wastes and wastewater management and other applications, a prime concern regarding GHs. The ultimate goal is the safe reuse of GH biomass that minimizes negative environmental footprint and provides resource recovery and reuse of waste biomass by transforming it into useful HC. Successful findings will allow inhouse reuse that matches nicely with global program objectives, as outlined in the WHO Guidelines [36]; contributing to a circular economy.

2. Sample Preparation and Experimental Procedures

Biomass carbonization using HTC was the main biomass valorization method used. Production of HC from tomato plant biomass required preparation to provide suitable feedstock to the HTC.

2.1. Sample Preparation and Analysis

Dead tomato plant biomass was collected from two local greenhouses through the Ontario Ministry of Agriculture, Food and Rural Affairs (OMAFRA). Tomato plant stems, internodes, nodes, and leaves, along with petioles, were sun-dried (for easy grinding), chopped into minimum sizes of 3–5 mm and then crushed in a grinder. The steps in material preparation are shown in Figure 1.



Figure 1. Biomass preparation steps for HTC process.

About 90.63% moisture (103 ± 2 °C) was estimated from biomass where leaves contain 88.69% moisture and nodes, and antinodes contain 93.93% moisture. Moisture content was determined from weight difference after overnight drying at 103 ± 2 °C. It revealed that nodes and antinodes contained more water compared to leaves, the stem contained an average of about 90.50% water. Feedstock was manually chopped into lengths ranging from 3–5 mm to prepare a more uniform sample. These prepared samples were then stored in a sealed plastic bag until treatment. The ground sample particle sizes were 49% (>500 μm), 42% (250–500 μm), 5.3% (100–250 μm) and 3.7% (<100 μm), respectively.

2.2. Carbonization by HTC Process

The HTC process was performed by mixing the biomass with deionized water and heating at 200–260 °C under autogenic pressure (2–5 MPa) for 5–60 min in the absence of air to get high carbon yield. About 10–30 g of ground sample was mixed with deionized water at different ratios 1:6–1:12 (biomass-water) and loaded into the HTC chamber. The added water acted as the carbonization medium. The HTC chamber was then closed, and pre-pressurized (100 psi) or simply purged with nitrogen (N_2). The HTC equipment was heated up at different target temperatures (200, 220, 230, 250 and 260 °C). Some of the experiments were conducted feeding with catalyst, or at controlled pH (acetic acid to maintain a pH of about 2.5–3.5 or KOH to a pH of 10.0–11.0). Figure 2 shows the photograph of experimental setup of the HTC equipment, along with a schematic flowchart summary of the process.

A unique advantage of the process is the elimination of the energy-intensive and costly pre-drying process. Reaction pressure was not controlled, it remained isotropic with vapor pressure of sub-critical water (water under pressure) corresponding to reaction temperature. The higher the sub-critical water temperature, the lower the dielectric constant of water behaving as an organic solvent, and thus of dissolved organics present in the biomass, along with metals, with the help of the acid generated during the process [37,38]. The final results were three products: solid hydrochar (HC), water soluble organics (process water), and trace amounts of gases (off gas). Reaction temperature (and pressure) determined the product distribution and proportion patterns. After reaching the desired temperature and duration, the reactor vessel was immersed in cold water cooled down to room temperature in about 5–7 min, which further quenched the reactions. Once the inside temperature of the reactor vessel reached room temperature, the pressure release valve was opened under the fume hood and the gaseous products were allowed to escape. The solid and liquid products were separated using micron filtration (11 μ) and collected for further analysis. The HC samples were dried overnight at 103 °C before further analysis. Each experiment was repeated three times to ensure reproducibility and consistency.

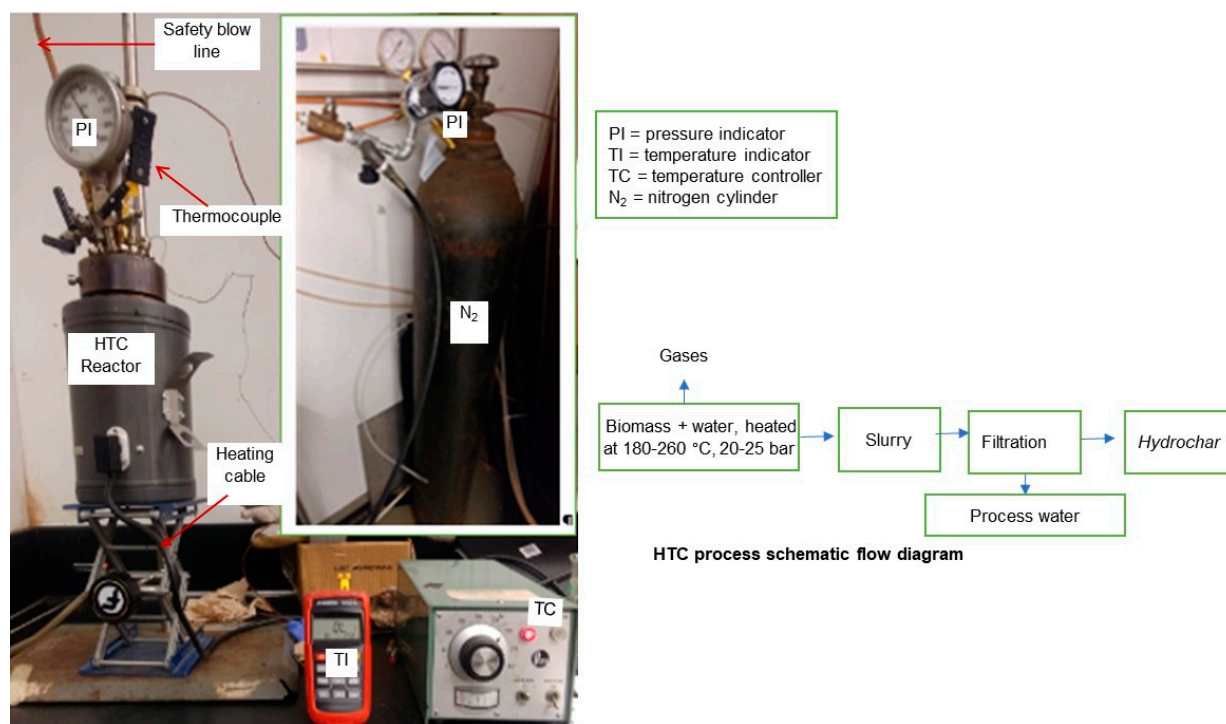


Figure 2. HTC components set-up along with schematic summary of the process.

2.3. Characterization

Experiments were performed for biomass *fiber analysis*, chemical analysis for metal detection, proximate analysis and ultimate analysis on the biomass and HC using standard methods. Calculation of *calorific values* for HCs and biomass, surface functionality assessment for HC, *thermal assessment* of HC degradation and further transformation on heating, and integrative *pyrolite identification* and quantification for HC were also completed. The latter three techniques (surface functionality, thermal, and pyrolite assessment) contributed in supplying supportive information for the next step of HC-activation by conventional heating pyrolysis. *Metal* detection was conducted using ion chromatography (IC) systems, which separated charged particles from digested liquid and measured their concentrations. Extraction of metals from biomass and HC were conducted by using digestion with royal water (HCl:HNO₃ molar ratio 3:1) under controlled temperature (90 °C), constantly stirred for two hours and then washed with DI water. Concentrations were obtained by using dilution factor and mass of sample used.

Proximate analysis was conducted using a muffle furnace applying standard methods: moisture (ASTM E1756), VM (ASTM E872), FC, and ash (ASTM E1755-01). The ultimate analysis was conducted using Thermo Fisher Scientific Flash (Mississauga, ON, Canada) 2000 Organic Elemental CHNS/O Analyzer. For surface functionality detection, *Fourier Transform Infrared spectroscopy (FTIR)* was obtained utilizing a Spotlight 200i FT-IR Microscopy (Thermo Scientific Nicolet 6700) System. A small amount of dried hydrochar was placed onto the crystal surface and secured. A total of 32 scans at a resolution of 4 cm⁻¹ were averaged to give the spectra for analysis. Spectrograph optical spectroscopy software Version 1.2.15 was used for the analysis of data and graphs.

Hydrochar pyrolite identification and quantification was conducted by using Gas Chromatography—Mass Spectrometry (GC-MS and Py-GC-MS) of Agilent 5977B GC/MSD. The *high heating value (HHV)* of HC was determined by IKA-C200 bomb calorimeter (IKA Works Laboratory Equipment, Washington, DC, USA). Estimation and comparative assessment of calorific values from biomass and HCs were conducted using a measured amount of dry sample (approx. 0.5 g), placed in the steel container of the IKA-C200 bomb

calorimeter fitted with a ceramic crucible, pressurized to 30 bars, and ignited with a cotton thread connected to the ignition wire in the decomposition vessel.

Thermal assessment of HC was conducted by Thermogravimetric analysis (TGA) using TGA-SDT Q600 (TA Instruments Waters LLC., New Castle, DE, USA). TGA was used to investigate the characteristic changes of HC on further heating under controlled conditions, and the physical and chemical phenomena were identified through analysis of thermal decomposition patterns. The weight loss percent at different stages of heating, temperature of exothermic and endothermic reactions, and percent derivative weight loss rates at various stages of temperature were assessed by TGA. Information on the fuel value of the HC sample, the temperature at which combustion started and ended, along with other characteristics, including reactivity temperature, ash amount, and total combustion time, were assessed from this analysis.

Biomass fiber materials were estimated using the following procedures: water-soluble materials present in the biomass were extracted by boiling 1.0 g of dried sample with 75 mL water for an hour, changing with fresh water and boiling again for one more hour followed by washing with cold water. Extractables were estimated by drying the residue at 60 °C for 16 h, taking the weight and getting the difference with the initial weight. *Lignin* was extracted by adding 2 mL of 10% acetic acid, and 0.6 g of NaCl, heating for 1 h at 75 °C, while additional acid (2 mL) and 0.6 g NaCl were added and continually heated to complete two hours. At this stage, the sample was washed 5 times with water, twice with acetone, and once with ether, and finally dried at 105 °C for 90 min and weighed to get the lignin extraction amount. *Hemi-cellulose* was determined by adding 20 mL of 24% KOH solution with the dried sample and allowed to react for 2 h at 20 °C, and finally the sample was washed for 5 times with water, once with 5% acetic acid, and once with each of water, acetone, and ether, prior to drying at 105 °C for 90 min and weighed to determine *hemicellulose* contents. The residue was assessed as *cellulose* after correcting for ash determined during proximate analysis. A similar technique was used by Wen et al. [39], while working with bamboo biomass, and Harper et al. [40] in the case of wheat straw leaves.

2.4. Statistical Assessment of Data

All the qualitative properties of each sample were determined statistically by applying a pooled variance two sample *t* test at $p = 0.05$ in order to determine if there was a statistical difference in their respective properties.

Multiple regression fitting assessment was used to find the best fitting of the coefficient of quadratic model of response variables. Use of significance test and analysis of variance (ANOVA) to qualify the fitted quadratic model was also employed to evaluate the cases of multiple independent and dependent variables. The type of fitted model is shown in Equation (1).

$$Y = a_0 + a_1x_1 + a_2x_2 + a_3x_3 + a_4x_1x_2 + a_5x_1x_3 + a_6x_2x_3 + a_7x_1^2 + a_8x_2^2 + a_9x_3^2 \quad (1)$$

where *Y* is the dependent variable, a_0 is the intercept, x_1 , x_2 , and x_3 are the first order coefficients, a_4 , a_5 and a_6 are the interaction coefficients a_7 , a_8 , and a_9 are quadratic coefficients, and x_1 , x_2 , and x_3 are independent variables.

Assessment of model, interpretation of coefficients and relation of dependent and independent variables were interpreted incorporating hypothesis testing and justification ($p = 0.05$). To exclude insignificant terms backward, an elimination procedure was applied.

3. Results and Discussion

Both physical and chemical characteristics of HCs were determined to assess how they contribute to valorizing the products. Fuel properties for both the biomass and HC were compared along with assessment of reduction in clinker formation in the generated HC fuels. Chemical catalyzation, or doping of functionals, for the improvement of fuel characteristics of some of the HCs were also interpreted. Greenhouse application of HC,

such as soil remediation to provide plant nutrient support, as well as nutrient concentration reduction in greenhouse nutrient feed (GNF) water, was also assessed to evaluate recycled uses of treated biomass within the facility itself. Experiments were conducted to assess components of waste TPB and produced HC. At a process temperature of 220 °C (max 260 °C) and corresponding pressures up to approximately 20–25 bar, very little gas (1–3%) was generated. The majority of the organics in solution were transformed into solids (adsorb on solid surface). Hydrochar was the main product with higher mass yield (50–75%) compared to biomass organics (25–35%) that remained in the process water. Off gases were very low and were not included in the assessment.

3.1. Experiments for Biomass Fiber Estimation

Fibers in TPB were estimated by sequentially extracting the components of biomass and weighing to assess the % presence of individual components through weight loss calculation. Tomato plant biomass metal analysis revealed about 76,900, 37,700, 4300, and 500 mg/L of K, Ca, Mg, and Na, respectively, a substantial reduction from biomass metal contents. Table 1 shows the respective results in terms of % of cellulose, hemicellulose, lignin, water soluble (extractives), and ash contents in the tomato plant biomass sample. Hemicellulose is a heteropolymer of pentose (xylose) and hexose sugars (galactose, glucose, mannose) linked through glycosidic bonds [9]. Extractives are composed of monomeric sugars (glucose, fructose), alditols (i.e., sugar alcohols), acids (aliphatic), oligomeric sugars (small part of polymer intermediate), and phenolic glycosides, known to be water soluble materials. Table 1 reveals a higher extractive (>14%) from tomato plant biomass when compared to miscanthus (6.6%) and switch grass (13.6%). Similarly, hemicellulose content (about 38%) was higher than the other two biomass samples, revealing that TPB is a low-quality biomass, as compared to the other biomasses.

Table 1. Fiber analysis results of tomato plant biomass in mass (%) and comparison with other biomasses.

Biomass	Extractives %	Hemicellulose %	Lignin %	Cellulose %	Ash %	HHV MJ/kg
Tomato plant	14.1 ± 2.4	37.2 ± 2.1	11.9 ± 1.8	32.1 ± 2.6	4.7 ± 0.3	12.7
Miscanthus [41]	6.9	30.2	14.2	44.4	4.4	17.4
Switch grass [41]	13.6	33.7	8.4	35.3	9.1	15.3
Corn stover [41]	26.3	26.3	9.5	29.7	8.2	15.6

The two other components of tomato plant biomass, lignin and cellulose, were lower than miscanthus. Consequently, tomato plants showed lower HHV values compared to miscanthus and switch grass. It can be mentioned here that the HHV values for lignin were the highest (23.3–26.6 MJ/kg) compared to hemicellulose and cellulose (15–18 MJ/kg), resulting in higher HHV values in miscanthus and switch grass, due to their higher lignin content. Cellulose is a homo polymer of glucose subunits, a polysaccharide of D-glucose linked through glycosidic bonds. Lignin is a high molecular weight cross-linked heteropolymer of three different phenyl-propane monomers groups [42]. Cellulose contains higher oxygen and lower C compared to lignin. Lignin has the opposite properties of highest carbon and lower oxygen. As C and H are considered as positive and O is a negative factor in heating value calculations, these parameters may also explain why the three biomasses noted in Table 1 have higher HHV values compared to tomato plant biomass. All the analyzed TPB sample parameters for cellulose, hemicellulose lignin, and ash were uniformly distributed ($p < 0.05$); significant to analysis accuracy. Further discussions on tomato plant biomass quality are included in the ultimate analysis (Section 3.3) along with elemental results of cellulose and lignin.

The obtained ash (%) from the 8 biomasses (*sunflower husk, oat husk, wheat straw, miscanthus, hay, wood chips, willow, and poplar*) were 4.09, 1.89, 1.70, 1.20, 5.70, 0.80, 1.45, and 4.70 (%), respectively [14]. TPB ash (4.70%) content was higher than almost all the biomasses, except Hay (5.70%) and Poplar (4.70%). Similarly, moisture (%) content in the 8

biomasses were 9.41, 11.76, 12.08, 11.83, 20.00, 40.00, 19.02, and 48.80 (%), respectively [14]. All of the biomass moistures were revealed to be below TPB (90.00%). The HHV (MJ/kg) from the 8 biomasses evaluated were 18.52, 16.58, 18.05, 18.91, 18.20, 19.40, 19.47, and 9.37 (MJ/kg), respectively [14]. Compared to TPB (12.70 MJ/kg) all the values were above TPB, except Poplar (9.73 MJ/kg). Overall, excepting Poplar, all the other 7 biomass qualities were revealed to be better than TPB.

Table 1 reveals hemicellulose (%), cellulose (%) and lignin (%) of Miscanthus, Switch grass, and Corn stover [41]. Hemicellulose in TPB (37.20%) was higher than Miscanthus (30.20%), Switch grass (33.70%), and Corn stover (26.30%). Lignin content of Switch grass (8.40%) and Corn stover (9.50%) were lower than TPB [41]. The miscanthus evaluated earlier [43] revealed hemicellulose (36.3%), cellulose (38.8%), and lignin (11.5%), which were different than the miscanthus [44]. It can be concluded that biomass qualities are location and time of sampling based.

3.2. Metal Contents in Plant Biomass and HCs

Chemical compositions of biomass and three different hydrochars were conducted to identify individual metal concentrations. Digestion at 90 °C was used to dissolve the measured quantity of sample completely and to extract metals from the HC and biomass materials, reviewing techniques used, in this respect, in other studies [45,46]. However, those studies conducted digestion on medicine products [45], and on mercury in herbal preparations [46]. As such, there was no literature observed by the author specific to lignocellulosic biomass assessment by royal water. Using available standards, four metals were analyzed by IC, and concentrations were back calculated into mg/kg using dilution factors of the individual samples. Energy dispersive X-ray spectroscopy (EDS) was used to assess for Ti, Si, Fe, Al and Cl contents in the HC. EDS revealed no trace of Ti, traces of Si (0.13%), Fe (0.305%), and Al (0.09%), which were insignificant related to ash. Almost all of them transferred from biomass to process water-reducing ash in HC. Table 2 shows the IC analyses of metal contents (Na, K, Ca, Mg) from the raw biomass and HCs along with % reduction of metals by HTC. Sulphur (%) was collected from elemental analysis. It revealed that each of the HCs and biomasses were leaching metals, based on severity in HTC conditions. Results showed that K was the highest in biomass, most probably originating from the high concentration of K in GNF as P transformation and precipitation of K is lower than for other metals. Also, component concentrations in an applied fertilizer are generally transmitted/reflected in the biomass. Sodium content was 0.5 g/kg, while K and Mg were 76.9 g/kg, and 4.3 g/kg, respectively, and Ca was about 37.7 g/kg in the biomass.

Table 2. Metal concentrations in biomass and three HCs including % removal.

	(mg/kg)				% Removal		
	HC at 260 °C	HC at 220 °C	HC at 250 °C NP	Biomass	HC at 260 °C	HC at 220 °C	HC at 250 °C NP
Na	396.5	395.1	585.7	500	20.7	21.0	
K	1586.0	5926.5	37,094.98	76,900	97.9	92.3	51.8
Mg	991.3	987.8	5857.1	4300	77.0	77.0	
Ca	5749.4	1461.9	8180.4	37,700	84.8	96.1	78.3
S%	0.0055	0.0069	0.031				

NP = nitrogen purge.

The reduction in concentrations by the HTC process varied from 20.7% to 97.9%. The highest reduction occurred with K metals followed by Ca and Mg. Sodium reduction was the least in the HCs. Water replaced toxic and corrosive agents, including metals, in the biomass that dissolved in water [47]. HTC subcritical water reduced Na by 20.7% at 260 °C, while K and Ca reduction ranged from 84.75% to 97.94% at 220 °C. These substantial

reductions show the great benefits of the HTC process. The leaching of metals from biomass to subcritical water contributes greatly to reducing agglomeration during fluidized bed combustion of HC compared to biomass. If these inorganics are not removed from the biomass, they end-up in the ultimate ash, causing fouling and slagging when used as fuels. Similar reduction of fouling and slagging indexes (medium to full) were observed from Corn Stover, Miscanthus, Switch grass, and Rich hull by hydrothermal treatment [41].

3.3. Quantitative Analysis of Biomass Fibers and HCs

In fuel characterization, the amount a material burns into a gaseous state from a fuel is termed volatile matters (VM), while the amount that burns into a solid state is termed fixed carbon (FC) and the % of inorganic waste materials that remain are termed ash. The VM, FC, and ash contents have fundamental importance in biomass energy, while FC has a positive relationship with charcoal yield, and both VM and ash have a negative relationship. The higher the VM in a biomass, the higher the gas yield at the expense of solid yield. Moisture is a rank indicator. The measurement of moisture, VM, FC, and ash contents constitute proximate analysis. In addition to proximate analysis, the other two basic parameters controlling fuel quality and technological behavior of a sample are the organic elemental composition (ultimate analysis) and high heating value (HHV). HCs at the different operating temperatures of HTC (220 °C, 230 °C and 260 °C) were all black. Visual observation showed that higher temperatures resulted in a blacker product, suggesting higher carbonization at higher temperatures. This was confirmed by elemental analysis. Mass (%) of C, H, N, and S were measured using organic CHNS/O analyzer. The O content was calculated after subtracting all the elemental percent and the ash by using the equation:

$$O\% = 100\% - (C\% + H\% + N\% + S\% + \text{ash}\%) \quad (2)$$

The two important atomic ratios, H/C and O/C were calculated using “mass %/atomic mass” of the respective elements and the well-known van Krevelen diagram was generated [48]. Figure 3 shows how the products behaved in comparison to typical carbon-based materials. Table 3 summarizes the results along with proximate data. For comparison, data on other biomass feedstocks, including HHV, are also included in Table 3. It should be mentioned here that the data in Table 3 are shown for one decimal; consequently, positions of H/C and O/C intersection points based on actual data values may look slightly different in Figure 3. For example, the O/C value for HC220-2 is 0.7 in Table 3, but the actual value is 0.67, shown in Figure 3. This also applies to other values as well (for example H/C values for HC220-1 and 2 are 1.26 each, but in Table 3 they are shown as 1.3).

Table 3. Proximate and ultimate analyses of tomato plant biomass and HCs compared with other biomass feedstocks.

Material	Moisture %	VM %	FC %	Ash %	C %	H %	N %	S %	O %	H/C	O/C	HHV (MJ/kg)
TPB	90.0	7.1	1.2	1.7	36.8	4.0	2.0	0.8	54.0	1.3	1.1	12.6 ± 1.2
Grass *	10.0–50.0	75.0–83.0	8.0–15.0	2.0–7.0	46.0–51.0	6.0–7.0	0.4–1.0	<0.02	41.0–46.0			16.0–18.7
A. Res. *	5.0–40.0	70–85	8.0–20.0	4.6–21.0	45.0–51.0	6.2–7.2	0.2–1.3	0.3–0.5	41–47			15.0–18.0
AA220 °C		89.7	9.3	1.0	50.9	5.6	0.9	0.1	41.5	1.3	0.6	18.6
220 °C (i)		93.9	5.2	0.9	47.8	5.1	1.4	0.2	44.6	1.3	0.7	18.0
220 °C (ii)		87.8	11.3	0.9	49.0	5.2	0.8	0.04	44.1	1.3	0.7	23.1
AA260 °C		86.8	12.5	0.7	50.6	5.6	0.8	0.06	42.2	1.3	0.6	25.9
np250 °C		88.7	9.1	2.2	44.6	3.7	3.1	2.0	44.4	1.0	0.7	17.4

Table 3. Cont.

Material	Moisture %	VM %	FC %	Ash %	C %	H %	N %	S %	O %	H/C	O/C	HHV (MJ/kg)
np230 °C		90.0	8.4	1.6	42.2	4.0	3.3	0.7	48.2	1.1	0.9	19.3
180 °C		85.3	13.5	1.1	43.4	5.4	1.2	0.1	48.8	1.5	0.8	17.9

Notes: * is from Reza et al. [49], aa = acetic acid; HHV = high heating value; (i) is batch 1, and (ii) is batch 2 of biomass supplies; A. Res. refers to agricultural residue, np refers to no nitrogen pressure.

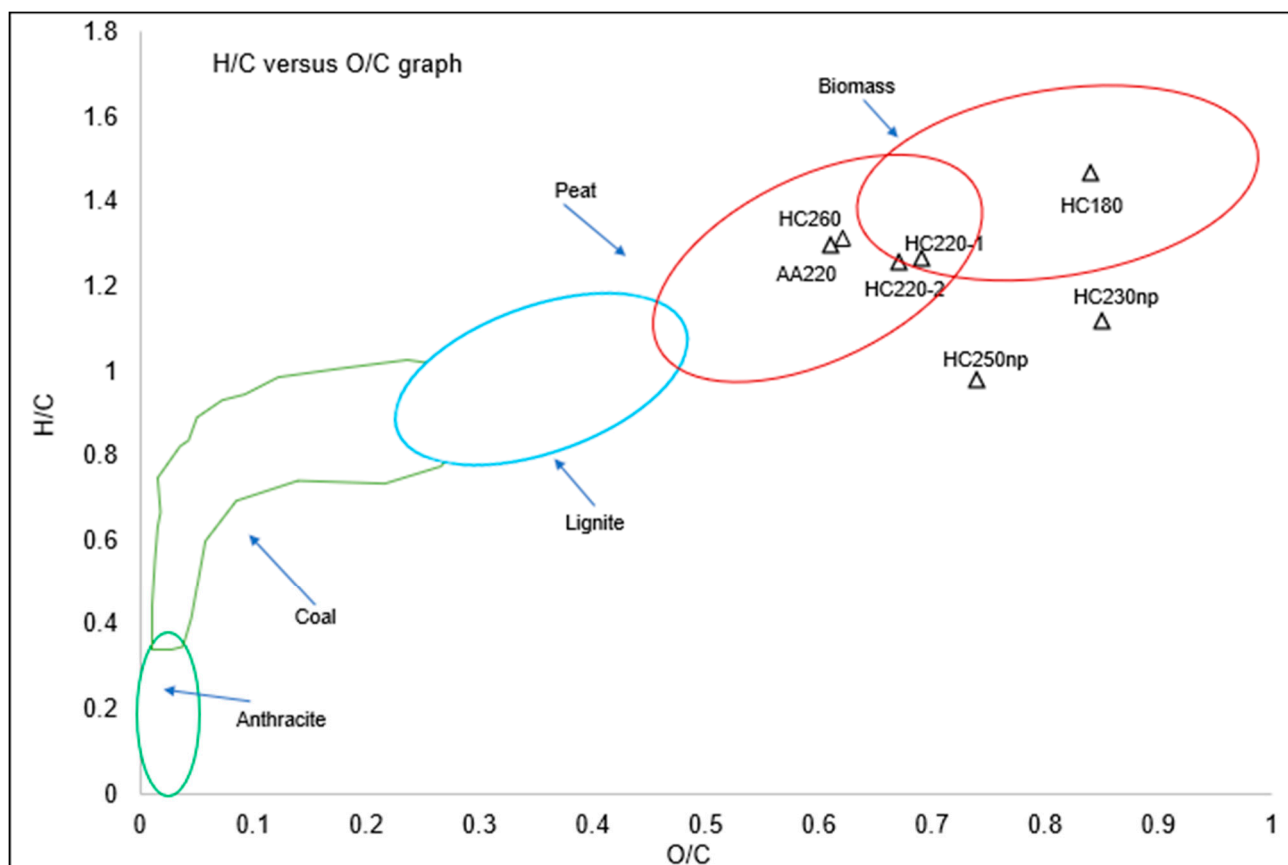


Figure 3. Van Krevelen diagram of hydrochars from tomato plant biomass.

An average solid yield after 90.0% moisture dried at 105 °C was 9.4% from TPB, where leaves contained 88.7% moisture and nodes and antinodes contained 93.9% moisture. This revealed that nodes and antinodes contain more water compared to leaves, while the stem contained an average of about 90.5% water. Both yields and elemental composition of derived HCs were greatly influenced by temperature. HC yields decreased with increasing temperature. Residence time had negligible impacts. The H/C and O/C ratio analysis revealed dehydration of biomass during HTC. Along with process severity, HC ash content was minimally changed. TPB C% (36.80%) was significantly lower than grass (C is 46.00–51.00%), agricultural residue (C is 45.00–51%) [50], and Miscanthus 46.70% [44]. This observation explains why TPB had a lower heating value, as lower carbon is one of the criteria for HHV. HTC temperature showed correlation (220–260 °C) with increased HHV to about 28% (dB), coefficient 0.18 (dB), ($p < 0.01$), and decreased ash content negatively to about 30% (dB), negative coefficient to -0.008 (dB), ($p < 0.01$). Other parameter changes were insignificant, except for fixed carbon (about 34%. $p < 0.01$). Statistically significant effects were revealed with HTC temperature in terms of HHV, ash, and fixed carbon. However, these observations cannot be generalized as biomass properties are site and material specific.

Figure 3 shows the positions of different char materials in H/C versus O/C graph. The labels AA220 and HC260 in Figure 3 are for the HCs when acidic (pH 3) DI water was used, the other 5 HCs were generated using normal DI water. Four of the HCs (HC260, AA220, 220 °C, and HC220-2) showed peat-like characteristics, while HC at 180 °C showed biomass-like characteristics, due to low transformation of biomass materials at <200 °C. Two HCs (HC230np and HC250np), operated at 230 °C and 250 °C, were generated from the latest two batches of biomass having more leaves compared to stem, nodes, and antinodes. These two biomass materials showed lower heating values at 230 °C and 250 °C. This is attributed to biomass quality, probably having more hemicellulose compounds. The nitrogen contents from these two HCs (3.11% and 3.25%) were high even after HTC treatment, when compared to TPB (2.01) %. Sulfur contents are also high. Higher nitrogen content revealed that the feedstocks contained higher protein (HHV 17.0 kJ/g) types of materials and less lignin, leading to lower heating values, high ash content, lower C % and higher O % even after carbonization.

In comparison to the other two biomasses (grass and agricultural waste), tomato plant biomass appeared to be a low-grade biomass, having very low carbon and hydrogen (and lignin as well) but higher oxygen content. Thus, it has a lower HHV (12.6 MJ/kg) compared to other biomasses, such as grass 16.0–18.7 MJ/kg. Generally, lignin-rich biomass shows higher HHV as lignin has higher HHV values (23.26 to 25.58 MJ/kg), higher C and lower O contents compared to cellulose [51]. HTC, an exothermal process, lowers both oxygen and hydrogen content from biomass mainly by dehydration and decarboxylation, which reduce H/C and O/C ratios. Similar behavior was observed with the tomato plant, where the H/C and O/C ratios reduced after HTC, although the uncarbonized biomass oxygen content was higher compared to other biomass feedstocks.

Results also revealed substantial increase of C from about 37 to 49%, and reduction of O from about 54 to 47% with hydrothermal treatment. Similar results were observed at an increase of temperature from 180 °C to 220 °C. There was a substantial increase of C content from 43.4% to 49.0%, and consequently H/C and O/C were reduced. Biomass composition plays a vital role at this stage, as interaction of cellulose, lignin, and hemicellulose, and their degradation products, are very complicated processes, and lead to the generation of various acids during HTC. For comparison, it was observed during pine and oak HTC, that the generated acids self-catalyzed the system and generated derivatives of 5-HMF, increasing the heating value of HC [52]. Results in the literature [49,53] have interpreted that most of the degradation of hemicellulose and lignin components, and the sorption of high heating value materials on the surface of HC was the reason behind the increase in the HHV value of HC. Similar results were observed in the present study. HHV results in Table 3 revealed that tomato plant dry biomass had the lowest HHV of 12.6 MJ/kg (within the range of 10–18 MJ/kg for biomass), which increased to 25.9 MJ/kg at HTC temperature of 260 °C. Also, it appeared that a HHV value of 18.4 MJ/kg at 220 °C increased to 19.2 at about 230 °C, with an increase of about 1 MJ/kg of HHV value. At lower temperatures the HHV value was improved by catalytic operations. For example, a HHV value of 18.6 MJ/kg was obtained at 220 °C and increased to about 23.1 MJ/kg at the same temperature of 220 °C when pH reduced by few drops of acetic acid (pH 3).

3.4. Functionalization of HC Materials

HC surface chemistry is very crucial and important to decide best use in the next step of further surface modification. To identify surface functionality, FTIR spectroscopy was used. Figure 4 shows the FTIR results of HC at 220 °C. Hydrochar generated at 260 °C was also compared, which revealed almost similar behavior with slightly higher peaks in the region of 1200–1600 cm^{-1} due to higher carboxylic acid (>COOH) and ketone formation at higher temperatures. The HC260 °C (acetic) and HC220 °C (non-acidic) operations reveal higher peaks at 1000–1150 cm^{-1} , which was assigned to -C-O- stretching. Acids (HC260 °C) were oxidized, and -COOH- functional stretching prevailed due to conversion of -C-O- into -C=O in the region of 1200–1700 cm^{-1} .

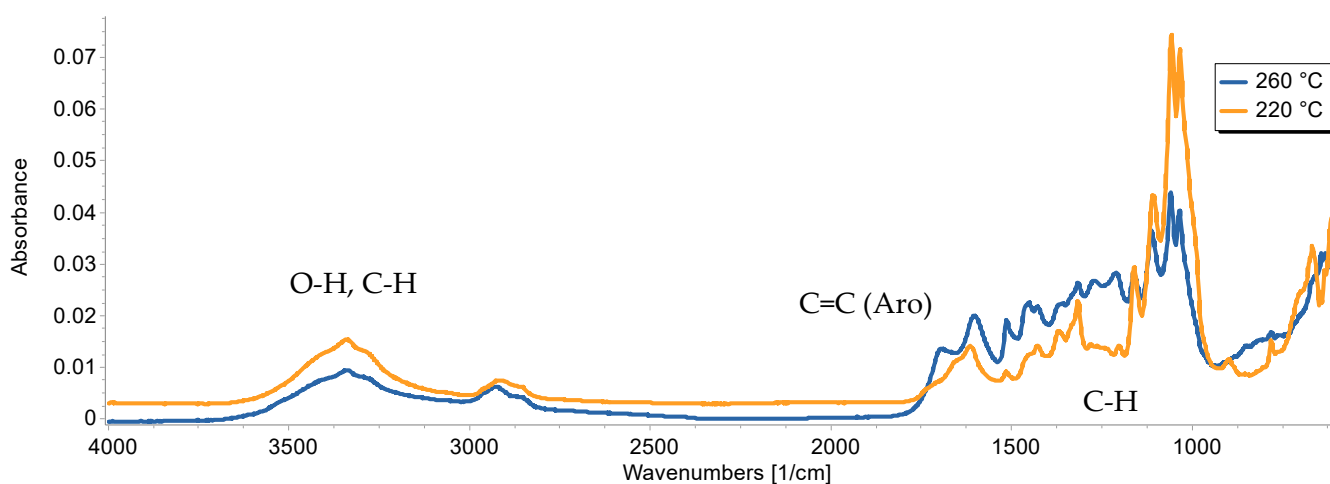


Figure 4. FTIR spectrograph of hydrochar produced at 260 °C and 220 °C.

The 1st wide peak at around 3200–3600 cm^{-1} can be attributed to the presence of -OH group stretching, alcoholic (aliphatic) or phenolic, or intermolecular hydrogen bonds in cellulose [54]. The second band (2800–2950 cm^{-1}) intensity at 2950 cm^{-1} was assigned to -CH₂- or -CH₃ which is related to the stretching vibration in alkyl or aromatic long linear chain fibers, and higher cellulose content in the case of HTC at 220 °C [55]. The region between 600–1720 cm^{-1} provides very interesting bands: bands at around 1720 to 1150 cm^{-1} were attributed to C=C vibration of structural aromatic rings, including C-H asymmetric vibration and deformation [36]. High bands around 1030–1114 cm^{-1} were assigned to deformation of C-H bonds in the aromatic rings along with deformation vibration of C-O bonds in primary alcohols and glycosidic (C-O-C) bond vibration [54,56]. Peaks at 1700 cm^{-1} represented stretching due to carbonyl (>C=O) or carboxyl (COOH) group compounds [57].

Spectral analysis revealed that HTC solid HC products contained polar oxygenated functionals, such as -OH, -COOH, and >C=O, which could be the target points for further functionalization through doping the required group (advanced carbon) or completely removing these functionals (activated carbon). The doping agent is exchanged with O functionals or with other group and improves HC quality. Also, it is known that removal or reduction of O will increase fuel calorific value, so interaction with O functional groups will improve calorific value as well. The contaminant adsorption capacity of HC, as well as its hydrophilic character, might also be improved through this process.

The most easy and beneficial use of the oxygen functional groups is in the activation of HC, where they help in pore formation reacting with, and removing, carrier gas at higher temperature treatment. All these positive impacts represent advantages of HTC in modification of surface chemistry with simple temperature treatment, which is otherwise very difficult to implement.

Oxygen containing functional groups on the surface of HC are supposed to enhance affinity for water, which can be used as water retention capacity in soil application. Polar surface functionalities and HC pyrolites analysis revealed scope for further promotion of the technology through post and in situ functionalization of HTC-HC into advanced carbonaceous materials. Study also revealed that application features of HC, surface functionality, morphological features, and reaction chemistry are affected by HTC operating conditions, manipulation of which would be the starting point for an advanced next study.

3.5. HC Pyrolites Analysis and Major Components Detection

To determine different substances within HC samples, Gas Chromatography-Mass Spectrometry (GC-MS and Py-GC-MS) analyses were performed using single shot flash pyrolysis of samples to produce gases to send through to the Py-GC-MS (Pyrolysis-GC-MS). The conditions of pyrolysis were at 500 °C for one minute, and GC was kept at 300 °C.

The analyzed data were integrated to obtain the peak areas by using F-search program. The areas (%) were identified and sorted with the help of Agilent Qualitative Analysis Software 10.0 and listed for comparison and interpretations. A total of 24 compounds were identified through the library search, which constituted about 80% of total substitutes. Out of 24 compounds, 11 pyrolites were sorted out as major compounds from the top listed concentrations and 13 compounds were found to have <2% concentration proportions. Table 4 shows a list of pyrolites, and Figure 5 shows the Py-GC/MS Total Ion Chromatogram (TIC) of the pyrolites, along with the respective names of the chemicals.

Table 4. List of pyrolite compounds from Py-GC-MS analysis of HC produced at 220 °C.

Chemical Name (Pyrolite Library)	Formula	MW	Ret. Time (min)		Com. %
			from	to	
Gas	CO ₂	44	1.7	1.765	11.41
Methyl glyoxal	C ₃ H ₄ O ₂	43	1.856	2.071	3.02
Hydroxy acetaldehyde	C ₂ H ₄ O ₂	31	2.064	2.401	11.48
Hydroxy acetone	C ₃ H ₆ O ₂	43	2.782	3.140	4.85
Hydroxyethyl acetate	C ₄ H ₈ O ₃	43	4.012	4.358	1.3
Succin-aldehyde	C ₄ H ₆ O ₂	29	4.113	4.513	3.46
2-Furfural	C ₅ H ₄ O ₂	39	5.079	5.148	0.97
3-Hexene-2,5-diol	C ₆ H ₁₂ O ₂	43		5.408	1.0
5-Methyl furan2(3H)-one	C ₅ H ₆ O ₂	98	5.806	6.211	2.37
Levoglucozan	C ₆ H ₁₀ O ₅	60	10.450	10.889	10.42
1-Tritriacontene (mixed with 1.32 and n-Tritriacontene)	C ₃₃ H ₆₆ , C ₃₃ H ₆₄	57	18.735	19.131	3.75
1-Hentetra-acontene(mixed with 1.40 hentetra-acontene)	C ₄₁ H ₈₂ , C ₄₁ H ₈₀	57	18.931	19.273	2.63
1-Hexatri-acontene (mixed with 1.35 and n-hexa-tri-acontene)	C ₃₆ H ₇₀ , C ₃₆ H ₇₄	57	22.231	23.05	6.24

3.6. Thermogravimetric Analysis (TGA) of HC

TGA was conducted following the procedure discussed earlier. Figure 6 shows the transformation of HC1 (220 °C) and HC2 (230 °C) on heating along with other TGAs from the literature for comparison. The thermal transformations that occurred in the 1st stage correspond to loss of moisture content up to 138 °C with a mass loss of about < 3.5% in the HCs, confirming the hydrophilic nature of the HCs. It was observed that most of the weight losses occurred in the 2nd temperature range, from 200–600 °C in the case of HC2, and 200–475 °C for HC1. After 600 °C (HC2) and 475 °C (HC1) there was no significant change of weight, even when the atmosphere changed from N₂ to air. Major decomposition, mainly of basic organic compounds, including hemicellulose (180–340 °C), cellulose (280–400 °C), and lignin (340–450 °C) took place. The weight loss was accompanied with the formation of CO₂, CH₄ and water vapor (reaction products) in the off gasses. The 2nd region represents decomposition of polymers, about 90% reduction of weight. The residuals were about 4% and 7% from HC2 and HC1, respectively. The 4th and 5th regions represent the combustion of carbon, and the remaining residuals are inert inorganic/filler materials.

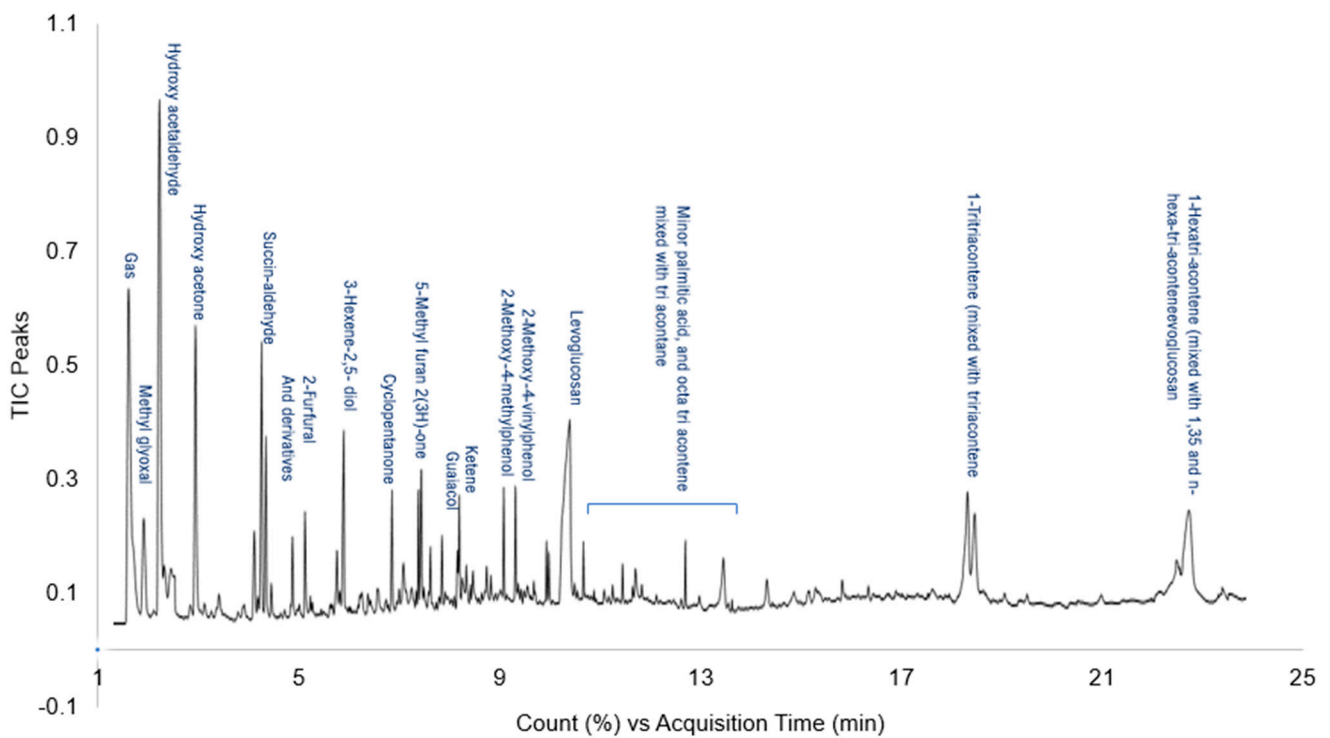


Figure 5. Major pyrolytes from HC of TPB.

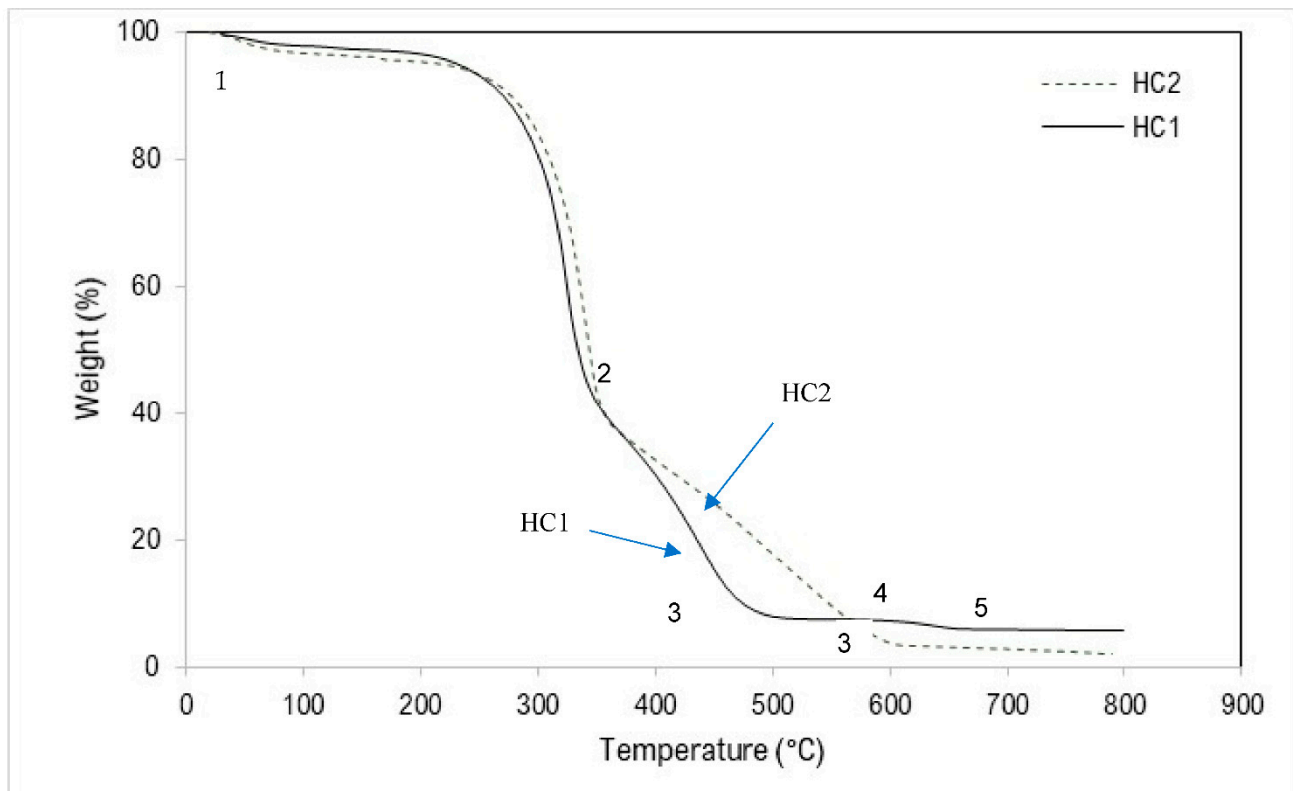


Figure 6. The TG physicochemical properties of HC1 (220 °C) and HC2 (230 °C) (10 °C/min, 50L/min N₂).

In comparison, olive residue provided about 35% yield, as compared to only 4–7% from the HCs. Only devolatilization occurred at 150 °C, followed by mixed weight loss at 300–350 °C, slower weight loss at 370 °C leading to about 70% total loss yielding about

30% residual from lignocellulosic wood materials [58]. Again, these results indicate lower quality TPB providing lower yields. Among the two HCs, HC1 provided better yields (7%), attributing to characteristics of biomass for this lot.

4. Applications of HC in GHs

As mentioned earlier HC could have multiple applications in science and engineering, including environmental sustainability. Two such applications, specific to the greenhouse from where biomass was collected, were verified in this research: (1) HC soil application for tomato seed germination, and plant nutrient supply and (2) HC in treatment of greenhouse leached nutrient feed (GNF) water, which is regulated and cannot be discharged without treatment.

4.1. Experiments on HC Soil Applications

Tomato seeds were collected from a ripped tomato supplied by one of the partner GHs and planted in a series of six small planting pots, mixing about 0.5–1.0% of HC (washed to free from acids) with potting soil in three pots in series (left) and the other three pots in another series left only with potting soil without any HC addition (right). Normal tap water (about 5 mL) was sprayed every alternate day. Figure 7 shows the results of the effects of HC addition.



Figure 7. Tomato planting pots (a) with and (b) without hydrochar. Above are seedlings which were planted in the pots.

After about 15 days, tomato seed germination occurred in both cases, but more germination occurred in pots amended with HC, as compared to pots not amended. Almost

all the 5–6 seeds germinated in pots with HC, while 2–3 seeds were weakly germinated in the pots without HC. After about 45 days, the seedling germinations were transplanted outdoors in two separate larger nursery plant pots with similar compositions of pot soil and HC mixing (with and without HC), and similar watering sequences (proportion to soil quantity). Within a month it was observed that the pot with HC was well-grown with tomato flowers, in comparison to the pot without HC. Figure 7 reveals the differences. The observation suggested that soil water retention and permeation was better in the pots with HC (both indoor seedling and outdoor planting) compared to without HC. The amendment helped in supplying and retaining nutrients in soil, improving soil physical and biological characteristics. Results proved that HC acted as conventional char or better, revealing similar benefits as already established by applying biochar in soil [59,60].

In addition to application for fuel and soil fertility, HC soil addition has various environmental benefits, such as carbon sequestration and greenhouse gas balance including: (i) carbon dioxide emission, (ii) nitrous oxide emission, (iii) methane emission. Other benefits, as proved with char application, are: (a) sorption of agrochemicals, (b) immobilization of heavy metals in contaminated soils, and (c) resistance against diseases. [59,60]. Table 5 summarizes remediation data including hydrochar source, soil type used, HC application rate, emissions, and residence time of use in cases of different biomass sources. The presented tomato plant biomass HC would be an addition to this database, although it is just a preliminary assessment without all the environmental evaluations, including GH gas balance. It may be included in an individual remediation study.

Table 5. Summary on hydrochar soil amendment at different experimental conditions using different biomass feedstock sources.

Feedstock	HC C Content (%)	Soil Type	HC Rate (g/kg Soil)	Emissions			Degradation Rate (%)	References
				CO ₂	N ₂ O	CH ₄		
TPB	47.8–50.5	Potting soil	5.0–10.0	n.d.	n.d.	n.d.	n.d.	Present work
Miscanthus	48.9	Inceptisol	3.4–9.7	n.d.	n.d.	n.d.	27–27	[61]
Corn silage	51.6	Arabian soil	5.2	+	–	++	>50	[62]
Bark	51.0	Oxisol	11.3	+	n.d.	n.d.	10	[63]
Glucose/yeast	64.6/67.4	Arabian soil	7.5	++	n.d.	n.d.	3–9	[64]
Beet root chips	49.7	Arabian soil	39.8	++	+	+	n.d.	[65]
Sugar beet pulp	49.2–52.5	Arabian soil	4.8–5.2	+	n.d.	n.d.	12–32	[66]

Notes: C is carbon; n.d. is not determined; + is 1 in 10; ++ is 10 time higher; – is decreased.

An important additional benefit of GH biomass HTC treatment is that HTC operations at >220 °C would obviously kill any plant pathogenic organisms in the biomass, making HC soil application safe and would resolve the issue of pathogens in GH. Based on the benefits, char materials are applied in different branches of science and engineering, including environmental science, agricultural and biological science, chemical engineering, chemistry, and others [67,68], while biochar produced by slow pyrolysis (torrefaction/carbonization) is well reported in soil application. At this stage, more extensive research with HC soil application is needed, including guidelines for HC production from various feedstocks with varied HTC parameters.

4.2. HC Application in Greenhouse Leached Nutrient Water Treatment

GNF water is regulated and restricted to land disposal after several uses. GNF contains high concentrations of nutrients, and its land disposal contributes to lake eutrophication and adversely impacts the environment. Therefore, GHs require proper treatment of GNF to reduce nutrients prior to disposal. Experiments were conducted to investigate the possibility of HC uses in adsorption of part of the nutrients from leached GNF. A known quantity of HC was added to the GNF and stirred for an hour and filtered to separate HC and suspended particles. The filtrate was then analyzed for nutrient contents. Ion chromatography was used for metal detection. Total nitrogen was analyzed following

the procedure TNT 826. Simplified TKN was analyzed following procedure TNT 880. Phosphorus, and reactive orthophosphate were measured by PhosVer 3 (Ascorbic Acid) Method 8048, Powder Pillow. The phosphate total was analyzed using TNT reagent 2742645CA. Table 6 shows the results.

Table 6. Treatment and % reduction of different nutrient from GNF by HC.

Parameters	GNF1 (mg/L)	HC Treated (mg/L)	% Reduction	GNF3 (mg/L)	HC Treated mg/L	% Reduction
NO ₃ & NO ₂ -N	226	202	10.62	319.5	238	25.51
TKN	231.5	211	8.86	165	128	22.42
TN (mg/L)	457.5	371	18.91	494.5	376	23.96
Phosphate total PO ₄ ⁻³	132	116	12.12	315	211	33.02
Phosphate reactive (orthophosphate)	67	60	10.45	175	151	13.71
Na	61	52	14.75	70	68	2.86
K	670	580	13.43	614	432	29.64
Mg	81	76	6.17	182	129	29.12
Ca	291	211	27.49	329	296	10.03

Results in Table 5 reveal a remarkable range of reduction (6–29%) of different nutrients from the two GNFs by HC (HC260 °C), while removal by other HCs produced at lower temperatures were lower. It is obvious that after activation of HC, the increased pore area and pore volume enhance HC nutrient removal capacity. Activation provides a more porous structure through the endothermic Boudouard reaction ($\text{CO}_2 + \text{C} \rightarrow 2\text{CO}$) that promotes porousness, and, hence, enhances sorption capacity. The reaction (>700 °C) of CO₂ with the organized organic structure of lignin-derived carbon generates pores [50]. Doping and/or impregnation of desired functionals on the surface of HC during HTC promotes surface modification and improves adsorption performance (chemical activation). The process involves dehydration, polycondensation, and gasification favoring low temperature activation. As a first-time study, it was significant that HC reduced nutrients from leached nutrient water.

Figure 8 shows a comparative SEM photograph of hydrochar before and after activation, which clearly reveal that activated carbon developed a more porous surface compared to HC. It can be mentioned here that commercially activated carbon (AC) showed about 40–69% reduction of nutrients from GNF. Comparatively, HC performance seems encouraging in having extra scope for improvements. Application features of HC, surface functionality, morphological features, and reaction chemistry are affected by HTC operating conditions, manipulation of which would be the starting point for a further study. Material and elemental analysis suggest a new strategy handling 2–3 types of waste biomass at a time, such as Co-HTC treatment of TPB together with other greenhouse biomass (e.g., cucumber and/or pepper plant). This provides a great opportunity for valued utilization of all types of waste biomass generated in greenhouses.

Material and elemental analysis suggested a new strategy handling 2–3 waste biomass at a time, which would provide additional benefits and could be a substitute to chemical doping. The high protein content biomass that can be in Co-HTC of TPB together with other greenhouse biomass (e.g., cucumber and/or piper plant) would provide a great opportunity for valued utilization of all types of waste biomass generated in a greenhouse. The present work concentrated on TPB to verify its applicability in recycle processes.

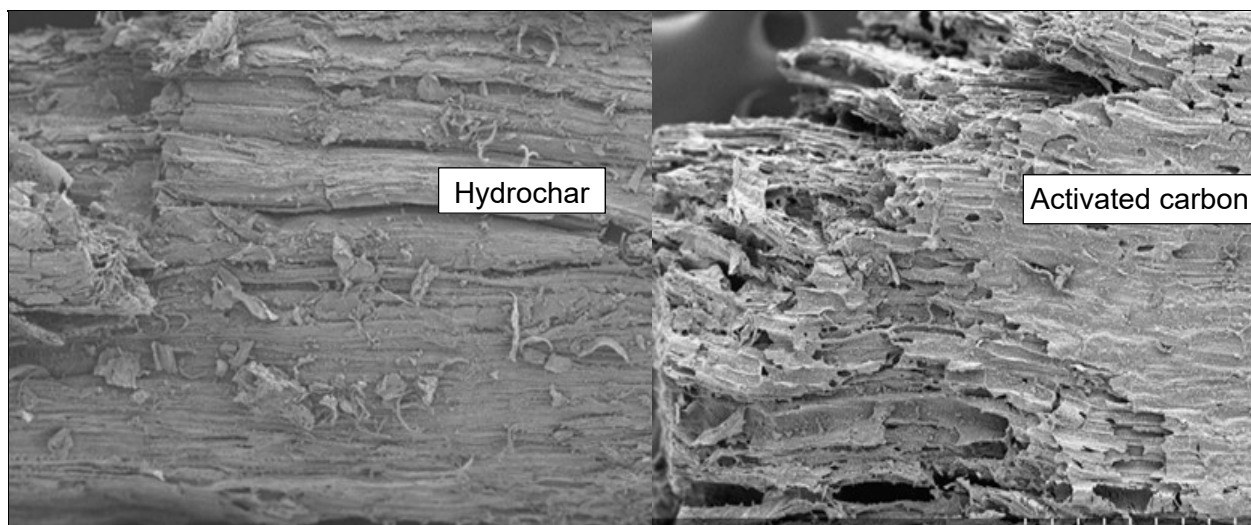


Figure 8. SEM-EDS of hydrochar before activation and activated carbon after activation.

Mixing low and high nitrogen content biomass, as well as doping with nitrogen (or oxygen) containing functional atoms on the surface of HC, can improve the quality of HC. Oxygen containing functional groups on the surface of HC enhances affinity for water, which can be used for water retention capacity in soil application [69]. The present work concentrated on tomato plant biomass to verify its applicability in recycle processes within the GH. Further development, partnering more GHs and HC soil application, is recommended as this application should be preferred over the use of HC as fuel.

5. Conclusions

Completion of the study with greenhouse waste and nutrient solutions has identified the following conclusions:

- Compared to the 12 other biomasses reviewed, TPB was revealed to be in the lower grade, in terms of HHV (MJ/kg) and moisture %. It may be in the rank of hay and poplar. TPB HHV was higher than poplar.
- Numerous beneficial uses of waste biomass were established: (a) HC for energy production, as high HHV values (25.9 MJ/kg) are comparable to peat and can be a fuel source for greenhouses or be a commercial commodity, (b) HC as fertilizer and soil ameliorant, (c) HC for GNF nutrient treatment.
- HTC substantially reduced inorganics from HC and lowered the slagging/fouling index of produced fuels; another benefit over other carbonizations.
- The uses of tomato plant HC in soil application and leached GNF nutrient reduction are new successes opening a door for biomass valorization and profit opportunity for greenhouses, along with providing environmental sustainability.
- More valuable advanced products, such as activated carbon and nanocomposites, seem to be possible from HC. Thus, HTC can play a vital role in production of nanostructured carbon; for example, N dopants may confer electronic as well as catalytic properties. Such an initiation for more advanced *HTC materials development* in future research would be a highly encouraging area.

Author Contributions: Conceptualization, R.G.Z., A.D. and A.-T.J.-U.; Methodology, A.-T.J.-U.; Software, A.-T.J.-U. and S.A.S.; Formal Analysis, A.-T.J.-U.; Investigation, A.-T.J.-U., S.A.S., A.D. and R.G.Z.; Resources, R.G.Z. and A.D.; Validation S.A.S., A.D. and R.G.Z.; Writing—Original Draft, A.-T.J.-U.; Reviewing and Editing, S.A.S. and R.G.Z.; Supervision, R.G.Z. and A.D.; Funding Acquisition, R.G.Z. All authors have read and agreed to the published version of the manuscript.

Funding: This research was funded by the University of Guelph through a general-purpose research account 070669.

Data Availability Statement: All data are included in the manuscript.

Acknowledgments: OMAFRA arranged supply of biomass and GNF from greenhouses. Shakir assisted with FTIR, TGA and CHNS-O analyses, Omid with GC-MS. All those contributions are highly acknowledged.

Conflicts of Interest: The authors declare no conflict of interest.

References

1. Bunch, K. Binational Plans Call for 40 Percent Reduction to Algal-Fueling Nutrients. 2018. Available online: <https://www.ijc.org/en/binational-plans-call-40-percent-reduction-algal-fueling-nutrients> (accessed on 22 April 2022).
2. Statistics Canada. Canadian Tomatoes, from Farm to Fork. 2022. Available online: <https://www150.statcan.gc.ca/n1/pub/11-627-m/11-627-m2021038-eng.htm> (accessed on 29 April 2022).
3. Nizamuddin, S.; Baloch, H.A.; Griffin, G.J.; Mubarak, N.M.; Bhutto, A.W.; Abro, R.; Mazari, S.A.; Ali, B.S. An overview of effect of process parameters on hydrothermal carbonization of biomass. *Renew. Sustain. Energy Rev.* **2017**, *73*, 1289–1299. [\[CrossRef\]](#)
4. Kambo, H.; Dutta, A. A comparative review of biochar and hydrochar in terms of production, physico-chemical properties and applications. *Renew. Sustain. Energy Rev.* **2015**, *45*, 359–378. [\[CrossRef\]](#)
5. Wang, R.; Wang, C.Z.; Zhao, Z.; Jia, J.; Jin, Q. Energy recovery from high-ash municipal sewage sludge by hydrothermal carbonization: Fuel characteristics of biosolid products. *Energy* **2019**, *186*, 115848. [\[CrossRef\]](#)
6. Shrestha, A.; Acharya, B.; Farooque, A.A. Study of hydrochar and process water from hydrothermal carbonization of sea lettuce. *Renew. Energy* **2021**, *163*, 589–598. [\[CrossRef\]](#)
7. Nanda, S.; Pant, K.; Naik, S. Characterization of North American lignocellulosic biomass and biochars in terms of their candidacy for alternate renewable fuels. *Bioenergy Res.* **2013**, *6*, 663–677. [\[CrossRef\]](#)
8. Yu, Y.; Lou, X.; Wu, H. Some recent advances in hydrolysis of biomass in hot-compressed, water and its comparisons with other hydrolysis methods. *Energy Fuels* **2008**, *22*, 46–60. [\[CrossRef\]](#)
9. Bobleter, O. Hydrothermal Degradation of Polymers Derived From Plants. *Prog. Polym. Sci.* **1994**, *19*, 797–841. [\[CrossRef\]](#)
10. Wang, D.; Czernik, S.; Chornet, E. Production of hydrogen from biomass by catalytic steam reforming of fast pyrolysis oils. *Energy Fuels* **1998**, *12*, 19–24. [\[CrossRef\]](#)
11. Isahak, W.N.R.W.; Mohd, H.; Yarmo, M.A.; Hin, T. A review on bio-oil production from biomass by using pyrolysis method. *Renew. Sustain. Energy Rev.* **2012**, *16*, 5910–5923. [\[CrossRef\]](#)
12. Kyoto Protocol Under the umbrella of “United Nations Climate Change”, Kyoto Protocol is a commitment of industrialized countries. **1997**, *11*, 1097. Available online: <https://unfccc.int/resource/docs/convkp/kpeng.pdf> (accessed on 29 June 2019).
13. Azarghor, D.; Nanda, S.; Dalal, A. Densification of Agricultural Wastes and Forest Residues: A Review on Influential Parameters and Treatments. In *Recent Advancements in Biofuels and Bioenergy Utilization*; Sarangi, P.K., Nanda, S., Mohanty, P., Eds.; Springer: Berlin/Heidelberg, Germany, 2018; ISBN 978-981-13-1307-3. [\[CrossRef\]](#)
14. Roman, K.; Barwicki, J.; Hryniewicz, M.; Szadkowska, D.; Szadkowski, J. Production of Electricity and Heat from Biomass Wastes Using a Converted Aircraft Turbine AI-20. *Processes* **2021**, *9*, 364. [\[CrossRef\]](#)
15. Jain, A.; Balasubramanian, R.; Srinivasan, M.P. Production of high surface area mesoporous activated carbons from waste biomass using hydrogen peroxide-mediated hydrothermal treatment for adsorption applications. *Chem. Eng. J.* **2015**, *273*, 622–629. [\[CrossRef\]](#)
16. Jiang, L.; Sheng, L.; Fan, Z. Biomass-derived carbon materials with structural diversities and their applications in energy storage. *Sci. China Mater.* **2018**, *61*, 133–158. [\[CrossRef\]](#)
17. Bargmann, I.; Martens, R.; Rillig, M.C.; Kruse, A.; Kücke, M. Hydrochar amendment promotes microbial immobilization of mineral nitrogen. *J. Plant Nutr. Soil Sci.* **2014**, *177*, 59–67. [\[CrossRef\]](#)
18. Chen, W.H.; Peng, J.; Bi, X.T. A state-of-the-art review of biomass torrefaction, densification and applications. *Renew. Sustain. Energy Rev.* **2015**, *44*, 847–866. [\[CrossRef\]](#)
19. Kan, T.; Strezov, V.; Evans, T.J. Lignocellulosic biomass pyrolysis: A review of product properties and effects of pyrolysis parameters. *Renew. Sustain. Energy Rev.* **2016**, *57*, 126–1140. [\[CrossRef\]](#)
20. Nicolae, S.A.; Au, H.; Modugno, P.; Luo, H.; Szego, A.E.; Qiao, M.; Li, L.; Yin, W.; Heeres, H.J.; Berged, N.; et al. Recent advances in hydrothermal carbonation: From tailored carbon materials and biochemicals to applications and bioenergy. *Green Chem.* **2020**, *22*, 4747–4800. [\[CrossRef\]](#)
21. Collard, F.-X.; Blin, J. A review on pyrolysis of biomass constituents: Mechanisms and composition of the products obtained from the conversion of cellulose, hemicelluloses and lignin. *Renew. Sustain. Energy Rev.* **2014**, *38*, 594–608. [\[CrossRef\]](#)
22. Funke, A.; Ziegler, F. Hydrothermal carbonization of biomass: A summary and discussion of chemical mechanisms for process engineering. *Biofuels Bio-Prod. Biorefin.* **2010**, *4*, 160–177. [\[CrossRef\]](#)
23. Jamal-Uddin, A.T.; Zytner, P.; Zytner, R.G. Hybrid Treatment System to Remove Micromolecular SMPs from Fruit Wastewater Treated with an MBR. *Can. J. Civ. Eng.* **2022**, *49*, 548–557. [\[CrossRef\]](#)
24. Tumuluru, J.S.; Christopher, T.; Wright, C.T.; Hess, J.R.; Kenney, K.L. A review of biomass densification systems to develop uniform feedstock commodities for bioenergy application. *Biofuels Bioprod. Biorefin.* **2011**, *5*, 683–707. [\[CrossRef\]](#)

25. Werpy, T.; Petersen, G. *Top Value Chemicals from Biomass*; US Department of Energy, Energy Efficiency and Renewable Energy, NREL: Washington, DC, USA, 2004; Volume 1, pp. 1–76. Available online: <http://www.ntis.gov/ordering.htm> (accessed on 13 April 2022).
26. Titirici, M.M.; Thomas, A.; Yu, S.-H.; Müller, J.-O.; Antonietti, M. A Direct Synthesis of Mesoporous Carbons with Bicontinuous Pore Morphology from Crude Plant Material by Hydrothermal Carbonization. *Chem. Mater.* **2007**, *19*, 4205–4212. [[CrossRef](#)]
27. Wang, T.; Zhai, Y.; Zhu, Y.; Li, C.; Zeng, G. A review of the hydrothermal carbonization of biomass waste for hydrochar formation: Process conditions, fundamentals.; physicochemical properties. *Renew. Sustain. Energy Rev.* **2018**, *90*, 223–247. [[CrossRef](#)]
28. Reza, M.T.; Rottler, E.; Herklotz, L.; Wirth, B. Hydrothermal carbonization (HTC) of wheat straw: Influence of feedwater pH prepared by acetic acid and potassium hydroxide. *Bioresour. Technol.* **2015**, *182*, 336–344. [[CrossRef](#)]
29. Yin, S.; Ryan, R.; Harris, M.; Tan, Z. Subcritical hydrothermal liquefaction of cattle manure to bio-oil: Effects of conversion parameters on bio-oil yield and characterization of bio-oil. *Bioresour. Technol.* **2010**, *101*, 3657–3664. [[CrossRef](#)]
30. Liu, L.; Neubauer, N.A. Gasification. In *High Temperature Processes in Chemical Engineering*; Lackner, M., Ed.; Process Engineering GmbH: Vienna, Austria, 2010.
31. Carter, B.; Gilcrease, P.C.; Menkhausy, T.J. Removal and Recovery of Furfural, 5-Hydroxymethylfurfural, and Acetic Acid from Aqueous Solutions Using a Soluble Polyelectrolyte. *Biotechnol. Bioenergy* **2011**, *108*, 2046–2052. [[CrossRef](#)]
32. Peterson, A.; Vogel, F.; Lahance, M. Thermochemical biofuel production in hydrothermal media: A review of sub- and supercritical water technologies. *Energy Environ. Sci.* **2008**, *1*, 32–65. [[CrossRef](#)]
33. Bergius, F. *Chemical Reactions under High Pressure*; 1991 Lecture Note; Nobel Foundation: Stockholm, Sweden, 1931; pp. 1–33.
34. Llorach-Massana, P.; Lopez-Capel, E.; Peña, J.; Rieradevall, J.; Montero, J.; Puy, N. Technical feasibility and carbon footprint of biochar co-production with tomato plant residue. *Waste Manag.* **2017**, *67*, 121–130. [[CrossRef](#)]
35. Savidov, N. Biochar: Growing a Sustainable Medium—Greenhouse Canada. 2019. Available online: www.greenhousecanada.com/technology-issues-growing-a-sustainable (accessed on 29 April 2022).
36. World Health Organization (WHO). *Guidelines for the Safe Use of Wastewater, Excreta and Greywater. Volume 2: Wastewater Use in Agriculture*; World Health Organization (WHO): Geneva, Switzerland; Food and Agriculture Organization of the United Nations (FAO): Rome, Italy; United Nations Environment Program (UNEP): Nairobi, Kenya, 2006.
37. Basso, D.; Casello, D.; Baratiri, M.; Flori, L. Hydrothermal Carbonization of Waste Biomass: Progress Report and Prospect. In Proceedings of the 21st European Biomass Conference and Exhibition, Copenhagen, Denmark, 3–7 June 2013; Available online: <https://www.researchgate.net/publication/257989805> (accessed on 29 April 2022).
38. Peter, K.; Eckhard, D. An assessment of supercritical water oxidation (SCWO): Existing problems, possible solutions and new reactor concepts. *Chem. Eng. J.* **2001**, *83*, 207–214. [[CrossRef](#)]
39. Wen, J.; Xiao, L.; Sun, Y.; Sun, S.; Xu, F.; Sun, R.; Zhang, X. Comparative study of alkali-soluble hemicelluloses isolated from bamboo (*Bambusa rigida*). *Carbohydr. Res.* **2011**, *346*, 111–120. [[CrossRef](#)]
40. Harper, S.H.T.; Lynch, J.M. The Chemical Components and Decomposition of Wheat Straw Leaves, Internodes and Nodes. *J. Sci. Food Agric.* **1981**, *32*, 1057–1062. [[CrossRef](#)]
41. Reza, M.T.; Lynam, J.G.; Uddin, H.M.; Coronella, C.J. Hydrothermal carbonization: Fate of inorganics. *Biomass Bioenergy* **2013**, *49*, 86–94. [[CrossRef](#)]
42. Saddawi, A.; Jones, J.M.; Williams, A.; Le Coeur, C. Commodity fuels from biomass through pretreatment and torrefaction: Effects of mineral content on torrefied fuel characteristics and quality. *Energy Fuels* **2012**, *26*, 6466–6474. [[CrossRef](#)]
43. Minaret, J.; Dutta, A. Comparison of liquid and vapor hydrothermal carbonization of corn husk for the use as a solid fuel. *Bioresour. Technol.* **2016**, *200*, 804–811. [[CrossRef](#)]
44. Kambo, H.S.; Dutta, A. Strength, storage.; combustion characteristics of densified lignocellulosic biomass produced via torrefaction and hydrothermal carbonization. *Appl. Energy* **2014**, *135*, 182–191. [[CrossRef](#)]
45. Uddin, A.H.; Khalid, R.S.; Alaama, M.; Abdulkader, A.M.; Kasmuri, A.; Abbas, S.A. Comparative study of three digestion methods for elemental analysis in traditional medicine products using atomic absorption spectrometry. *J. Anal. Sci. Technol.* **2016**, *7*, 6. [[CrossRef](#)]
46. Ang, H.; Lee, K.L. Analysis of mercury in Malaysian herbal preparations: A peer-review. *J. Med. Biomed. Sci.* **2005**, *4*, 1–6. [[CrossRef](#)]
47. Kruse, A.; Dahmen, N. Water—A magic solvent for biomass conversion. *J. Supercrit. Fluids* **2015**, *96*, 36–45. [[CrossRef](#)]
48. Van Krevelen, D.W. Graphical-statistical method for the study of structure and reaction processes of coal. *Fuel* **1950**, *29*, 269–284.
49. Reza, M.T.; Andert, J.; Wirth, B.; Busch, D.; Pielert, J.; Joan, G.; Lynam, J.; Mumme, J. Hydrothermal Carbonization of Biomass for Energy and Crop Production. *Appl. Bioenergy* **2014**, *1*, 11–29. [[CrossRef](#)]
50. Contescu, C.; Adhikari, S.; Gallego, N.; Evans, N.; Biss, B. Activated Carbons Derived from High-Temperature Pyrolysis of Lignocellulosic Biomass. *J. Carbon Res.* **2018**, *4*, 51. [[CrossRef](#)]
51. Demirbas, A. Relationships between lignin contents and heating values of biomass. *Energy Convers. Manag.* **2001**, *42*, 183–188. [[CrossRef](#)]
52. Menegazzo, F.; Elena Ghedini, E.; Signoretto, M. 5-Hydroxymethylfurfural (HMF) Production from Real Biomasses. *Molecules* **2018**, *23*, 2201. [[CrossRef](#)] [[PubMed](#)]
53. Kambo, H.; Dutta, A. Comparative evaluation of torrefaction and hydrothermal carbonization of lignocellulosic biomass for the production of solid biofuel. *Energy Convers. Manag.* **2015**, *105*, 746–755. [[CrossRef](#)]

54. Bykov, I. Characterization of Natural and Technical Lignins Using FTIR Spectroscopy. Independent Thesis. 2008. Available online: <http://www.diva-portal.org/smash/get/diva2:1016107/FULLTEXT01.pdf> (accessed on 23 June 2021).
55. Wang, W.; Chen, W.; Jang, M.-F. Characterization of Hydrochar Produced by Hydrothermal Carbonization of Organic Sludge. *Future Cities Environ.* **2021**, *6*, 13. [[CrossRef](#)]
56. Santos, J.I.; Fillat, U.; Martin-Sampedro, R.; Ballesteros, I.; Manzanares, P.; Ballesteros, M.; Eugenio, M.E.; Ibarra, D. Lignin-enriched Fermentation Residues from Bioethanol Production of Fast-growing Poplar and Forage Sorghum. *Bioresources* **2015**, *10*, 5203–5214. [[CrossRef](#)]
57. Miliotti, E.; Rosi, L.; Bettucci, L.; Lotti, G.; Maria Rizzo, A.; Chiaramonti, D. Characterization of Chemically and Physically Activated Carbons from Lignocellulosic Ethanol Lignin-Rich Stream via Hydrothermal Carbonization and Slow Pyrolysis Pretreatment. *Energies* **2021**, *13*, 4101. [[CrossRef](#)]
58. Colomba, A. Production of Activated Carbons from Pyrolytic Char For Environmental Applications. Ph.D. Thesis, University of Western Ontario, London, ON, Canada, 2015.
59. Elad, Y.; David, D.; Harel, Y.; Borenshtein, M.; Kalifa, H.; Silber, A.; Graber, E. Induction of systemic resistance in plants by biochar, a soil-applied C sequestering agent. *Phytopathology* **2010**, *100*, 913–921. [[CrossRef](#)]
60. Elad, Y.; Cytryn, E.; Harel, Y.; Lew, B. The biochar effect: Plant resistance to biotic stresses. *Phytopathol. Mediterr.* **2012**, *50*, 335–349. [[CrossRef](#)]
61. Bai, M.; Wilske, B.; Buegger, F.; Esperschütz, J.; Kammann, C.; Eckhardt, C. Degradation kinetics of biochar from pyrolysis and hydrothermal carbonization in temperate soils. *Plant Soil.* **2013**, *372*, 375–387. [[CrossRef](#)]
62. Malghani, S.; Gleixner, G.; Trumbore, S.E. Chars produced by slow pyrolysis and hydrothermal carbonization vary in carbon sequestration potential and greenhouse gases emissions. *Soil Biol. Biochem.* **2013**, *62*, 137–146. [[CrossRef](#)]
63. Qayyum, M.F.; Steffens, D.; Reisenauer, H.P.; Schubert, S. Kinetics of carbon mineralization of biochars compared with wheat straw in three soils. *J. Environ. Qual.* **2012**, *41*, 1210–1220. [[CrossRef](#)] [[PubMed](#)]
64. Steinbeiss, S.; Gleixner, G.; Antonietti, M. Effect of biochar amendment on soil carbon balance and soil microbial activity. *Soil Biol. Biochem.* **2009**, *41*, 1301–1310. [[CrossRef](#)]
65. Kammann, C.; Ratering, S.; Eckhard, C.; Müller, C. Biochar and Hydrochar Effects on Greenhouse Gas (Carbon Dioxide, Nitrous Oxide, and Methane) Fluxes from Soils. *J. Environ. Qual.* **2012**, *41*, 1052–1066. [[CrossRef](#)] [[PubMed](#)]
66. Gajić, A.; Ramke, H.G.; Hendricks, A.; Koch, H.J. Microcosm study on the decomposability of hydrochars in a Cambisol. *Biomass Bioenergy* **2012**, *47*, 250–259. [[CrossRef](#)]
67. Perez-Mercado, L.; Lalandera, C.; Joel, A.; Ottoson, J.; Dalahmeh, S.; Vinneråsa, B. Biochar filters as an on-farm treatment to reduce pathogens when irrigating with wastewater-polluted sources. *J. Environ. Manag.* **2019**, *248*, 109295. [[CrossRef](#)]
68. Lehmann, J.; Joseph, S. *Biochar for Environmental Management: Science, Technology and Implementation*, 2nd ed.; Taylor & Francis Group: Abingdon, UK, 2015; 994p.
69. Sevilla, M.; Maciá-Agulló, J.A.; Fuertes, A.B. Hydrothermal carbonization of biomass as a route for the sequestration of CO₂: Chemical and structural properties of the carbonized products. *Biomass Bioenergy* **2011**, *35*, 3152–3159. [[CrossRef](#)]